Adaptive ANN-Based Control Framework for High-Performance Hybrid Electric Vehicle Charging

Dr. K. Srinivas[1], M. Karunya[2]

[1]Professor, Department of Electrical and Electronics Engineering, JNTUH University College of Engineering (Autonomous), Jagtial Dist., Telangana, India.

[2]PG, M.Tech (Electrical Power Systems), Department of Electrical and Electronics Engineering,JNTUH University College of Engineering (Autonomous), Jagtial Dist., Telangana, India.

Abstract: ***It may take more time than needed to charge an electric vehicle (EV) using the onboard Type-1 and Type-2 AC chargers since their capabilities are often lower, ranging from 3.3 kW to 19 kW. The construction and maintenance of off-board high-power DC fast-charging stations are costly, but they allow for quick charging. This research recommends a hybrid AC-DC charging method to get over these limitations and charge EV batteries faster. This vehicle is very easy to charge because to its Type-2 AC charger and built-in DC charger. Making ensuring charging happens successfully is as simple as following the setup instructions. One way to add a DC input port to an electric vehicle is to connect the motor windings' neutral point to the drivetrain inverter's negative rail. This connection makes it possible to directly link to various renewable energy sources, such as DC microgrids, rooftop solar panels, and electric vehicle batteries. To improve power conversion, the electric vehicle's drivetrain inverter may mimic an integrated interleaved DC-DC converter by using the motor windings as filter inductors. It replaces the conventional PI controller with an ANN-based one to increase control efficiency. In various operating conditions, this controller regulates the DC-link voltage and the power flow between the AC and DC charging channels. The whole system is tested and assessed using MATLAB/Simulink under different charging circumstances.***

Keywords_ Electric vehicle (EV) battery charging strategies, DC-Link voltage control, interleaved DC-DC converters, DC fast charging, Type-2 AC chargers

I. INTRODUCTION

Air pollution, climate change, and the loss of fossil fuels are just a few of the reasons why more and more people are looking for environmentally friendly ways to get about. The vast bulk of urban areas' pollution and greenhouse gas emissions originate from ICE-powered vehicles. The improved efficiency of transferring energy into useable form, decreased operating costs per km, and elimination of exhaust pollutants have made electric autos a realistic choice. Due in large part to developments in electric powertrain, power electronics, and battery technology, the popularity of electric vehicles (EVs) has skyrocketed since their launch. But there are still a lot of things standing in the way of EVs being extensively utilised, even with all these advantages. There are a lot of problems, the most important of which being long charging periods, little driving range, and old charging infrastructure. Although the increased energy density of batteries has increased the range of vehicles, charging times continue to be a major issue for consumers. Creating efficient and flexible charging infrastructure is crucial for expanding access to electric vehicles. Currently, electric vehicle charging stations that are located off-board provide faster charging times than on-board AC power sources. A medium-sized electric vehicle's battery may be fully charged in around 6-12 hours using an on-board AC charger of the Type-1 or Type-2 kind, with capacities ranging from 3.3 kW to 19 kW.A very long time is required to charge these small and inexpensive chargers due to their low power rating. Charging power at DC fast and ultra-quick stations, on the other hand, may range from tens to hundreds of kilowatts, drastically cutting down on charging times. Given the high grid capacity, huge installation space requirements, and considerable capital investment demands of these stations, residential and semi-urban regions are at a distinct disadvantage when using them.

To get over these restrictions and increase the charging speed for electric vehicles, a lot of innovative ideas have been put forth that don't depend only on pricey off-board fast chargers. The integrated AC/DC charging system of electric vehicles is one such solution. The battery is charged using this system's traction inverter and motor windings. By using their high-power capabilities, this strategy maximises the use of the vehicle's internal components. This makes rapid charging a better and more efficient choice in terms of space. The generation of charging torque is a significant obstacle to drivetrain-integrated charging. When a motor is charged with three-phase AC current via its windings, it generates a rotating magnetic field, which might cause the rotor to move in an unexpected way. Minimising or removing this charging torque is crucial since electric car charging must occur when the vehicle is at rest. Reducing torque output while charging has been suggested using a variety of methods. The use of mechanical clutch systems, rewiring of motor windings, and conversion to single-phase AC charging are all examples of such changes. A second workable option is to provide direct current (DC) to the stator windings; this will create a static magnetic field that stops the rotor from turning. In order to do this, the motor's neutral gear is used.

The dual-source possibility has been surprisingly under-discussed in the mountain of material on AC or DC drivetrain-integrated charging. Residential and commercial hybrid AC/DC power infrastructures have become the norm due to the widespread use of renewable energy sources, battery storage systems, solar photovoltaic installations, and DC microgrids. Unfortunately, current EV charging standards like CCS-2 and IEC 61851-2 do not permit the simultaneous use of separate AC and DC charging ports.

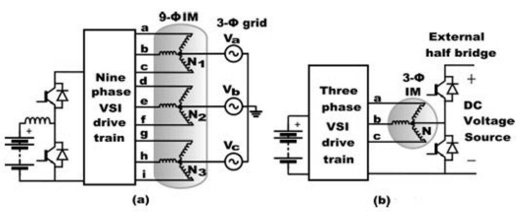

Fig. 1. Drivetrain integrated on-board EV charger configurations proposed in (a) [14] and (b) [15] using EV motor's stator winding neutral.

The research proposes a hybrid AC-DC EV charging system that might utilise both AC and DC power sources simultaneously to get around this limitation. The end outcome would be an increased overall rate of billing. The proposed approach states that building separate fast-charging infrastructure is more expensive than reusing the on-board charger and power circuits. By connecting the motor windings' neutral point to the negative rail of the drivetrain inverter, electric cars may connect to various direct current (DC) sources, such as industrial solar plants, battery storage systems, rooftop photovoltaic systems, and other EV batteries. The suggested charging system's control performance is enhanced using an ANN-based controller. Under all operating conditions, an ANN controller may replace the present PI-based control system to manage the DC-link voltage and coordinate the power flows between the AC and DC charging pathways. Thanks to the ANN controller's adaptive learning and nonlinear mapping capabilities, the system becomes more responsive, stable, and efficient while charging.An interleaved DC-DC converter's filter inductor is a good analogy for the drivetrain inverter. The efficacy of the power conversion is enhanced, and the charging power is proportionate to the DC source's capacity. The 45 kWh battery pack is compared in Table I using a number of criteria, including charging power level, charging flexibility with AC and DC sources, and maximum possible charging rate (C-rate). The results show that the proposed hybrid AC/DC charging system is faster and more flexible than the existing methods.

II. PROPOSED COMBINATORY AC AND DC EV CHARGING

Type-1 and type-2 ac chargers are often seen on EVs; they enable the cars to connect to single-phase and three-phase ac grids, respectively. Quickly top up your batteries with high-power DC current with the CHAdeMO adapter. However, the CCS2 Combo charging connector is most often used for commercial electric vehicles. By connecting the type-2 ac input and the CHAdeMO dc ports, a single intake may be used. You don't need to plug in your electric vehicle. On the battery side, you'll find powertrain inverters and dc-dc converters that have enormous output powers. Under normal driving circumstances, the dc-link level is achieved by boosting the power provided to the drivetrain inverter via the battery side dc-dc converter. Since the inverter is directly linked to the batteries, an on-board dc-dc converter is unnecessary in electric vehicle powertrain systems that employ internal permanent magnet motors (IPMs). Based on these findings, electric car designs that include a dc-dc converter onto the battery side of the vehicle might result in better mode control for IMmotor and IPM powered electric vehicles. The power architecture of electric vehicles (EVs) for passenger cars is shown in Figure 1, a block diagram, which shows the components that comprise it. A combination of alternating current (ac) and direct current (dc) is used by the charging system for hybrid electric cars, as seen in Figure 2. An additional DC input port (N (+), O(−)) that could receive power from a wider range of DC sources has been suggested as a method to enhance the electric car. The negative terminal (O(−)) of the drivertrain inverter is connected to the neutral terminal (N(+)) of the motor via this interface. There are a number of options for powering the drivetrain inverter. One way is to link it to external direct current sources. The electric motor's stator windings serve as interleaved filter inductors in addition to regulating the drivetrain inverter. Thanks to the built-in type-2 charger, charging the electric vehicle is a snap. Through its integrated interleaved dc-dc converter, you may power it from either the alternating current (ac) grid or direct current (dc) sources, or even a combination of the two. In the suggested integrated billing approach, each of these three possibilities is considered.

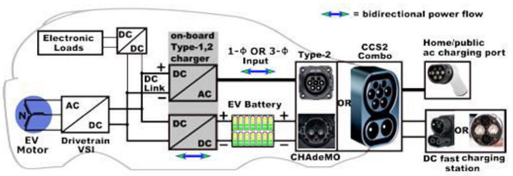

Fig.2 Power architecture showing drive train, EV motor, on-board power converters with power input ports of an EV.

A three-phase active rectifier is required for a type-2 charger to function. The dc-link on an EV's powertrain is where it connects for dc output. The built-in interleaved, battery-side, and regulated rectifier dc-dc converters also make use of the dc-link.To minimise current cycling between the controlled rectifier and interleaved dc-dc converter outputs, which is critical for the proposed mixed ac and dc charging, it is important to maintain a constant dc-link voltage. On the battery side, the controlled rectifier and integrated interleaved dc-dc converters provide the charging current, while the dc-link controls the voltage from these sources. By taking power from the dc input voltage (VdcE) attached to the dc input port, the IDC raises the voltage at the dc-link terminal. The top diodes D7, D9, and D11 will be biassed forward if VdcE surpasses the dc-link voltage, which happens when the dc-link voltage is higher than its rated value. The dc-link, on the other hand, is ideal for use in electric vehicle drivetrains due to its high rated value (>600V) and wide voltage range (170-500V). The DC input port of the integrated IDC may be connected to a number of standard DC voltage sources, making it possible to charge electric automobiles. Rooftop solar panels, direct current microgrids, and energy storage devices are all instances of such sources. The integrated DC drivetrain enables faster battery charging due to the electric vehicle's motor and inverters' ability to manage high power levels. A DC source's rating might be very low or high, depending on the situation. The V2V energy sharing architecture shown in [22] allows cooperative energy sharing between EV users via the use of a fast charging power interface. Power may be drawn from a wide variety of electric car batteries (350 V to 450 V) using a dc input port on the proposed integrated IDC.

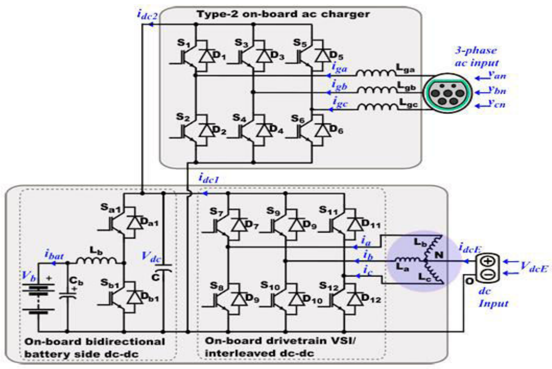

Fig.3 Detailed circuit diagram of the proposed combinatory ac and dc charging approach

III. CONTROL STRATGAGY

Any hybrid ac/dc charging system must include a bidirectional dc-dc converter and an onboard type-2 charger (IDC).A dc-dc converter and active rectifier are often mounted on the battery side to control the voltage and current during type-2 ac charging. The active rectifier's output power stays at the specified constant level, and the dc-link voltage stabilises at 600 V. If the control states of the active rectifier's type-2 charging and integrated dc charging are the same, it is feasible to disrupt its constant power functioning. In a hybrid ac/dc charging mode, this happens because the charging rate is exactly proportional to the required current reference. At the same time that the active rectifier, integrated rectifier circuit (IDC), and battery-side direct current to direct current converter are all running, our control system is able to produce a constant power output. The dc-link voltage must to remain at 600 V. A. When travelling with an AC charger type 2, it is recommended to keep the onboard charger in continuous power mode due to the higher maximum power ratings. One essential goal of AC charging management is to keep the grid's unity power factor (UPF) stable.Using d ∏ q and setting the reactive current reference i∏ q to zero is the suggested method for the UPF to handle the type-2 three-phase onboard charger and fulfil these two criteria. One way to use the battery-side voltage control mode of the dc-dc converter is to change the dc-link voltage needed for the active rectifier's UPF to work. All of the power for this device comes from an internal battery. The Pac output power, which is calculated as (idc1 ∏ Vdc), may be compared to the required average output power reference, P∏ ac. A compensator generates the active current reference, i∏ d, once the difference has been determined. The type-2 onboard AC charger produces power up to 19.4 kW, which is the maximum reference power. The details of the d − q control used in the type-2 onboard ac charging system are shown in Figure 4.

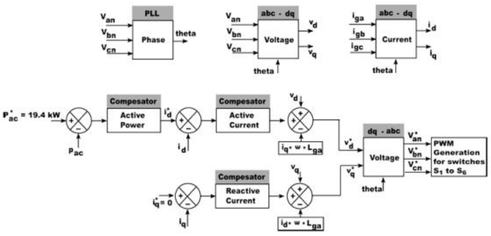

Fig. 4 Controller for unity power factor operation for the onboard type-2 ac charging using d − q control.

Interleaving DC-DC converters B. Inverter Control for the Drivetrain The electric vehicle motor's phase windings, or leg inductors, regulate the current flowing through them in relation to a current reference, i∏ l, as stated in (1). The drivetrain inverter is operated by a dc-dc converter with interleaved control. Finding the reference requires knowing the input dc source's power rating (PdcE). You may get the duty ratio for the integrated interleaved dc-dc converter's switches S8, S10, and S12 by comparing the current in each leg (ia, ib, and ic) with i∏l and then feeding the result into a compensator.The current-to-control transfer function is given in (2) so that the current compensator may be constructed. Figure 5 (a) shows the current error correction compensator and IPWM controller. The current compensator output and three phase shifted carriers are used to determine the required boost duty ratio in order to create switching pulses for the three legs of the integrated interleaved dc-dc converter. An interleaved dc-dc converter's output current ripple may be mitigated with the use of IPWM. When an electric car is charging, its motor windings act as filter inductors, allowing the interleaved dc-dc converter to pass high-frequency dc currents over the air gap without creating a spinning magnetic field.

$$i_{l*} = \frac{P_{dcE}}{3 * V_{dcE}} \quad (1)$$

$$\frac{\widehat{I_a}(s)}{\widehat{d_1}(s)} = \frac{(C_1 V_{dc})s + 2(1 - D_1)L_a}{(L_a C_1)s^2 + \frac{L_a}{R_2}s + (1 - D_1)^2} \quad (2)$$

A DC-DC converter is mostly used for battery charging. You may change the voltage by connecting the dc-link's input to the battery terminals and the bidirectional dc-dc converter. The only thing needed is a voltage-stabilized working mode. The dc-link voltage on the battery side of the dc-dc converter controls both the type-2 ac charger and the interleaved dc-dc power sharing for the drive train. The preceding sections provided evidence of this. Control the rate of rotation of the switch. If we compare the 600V VRDS with the measured dc-link voltage Vdc, we see that both Sa1 and Sa2 are covered. This is when the compensator comes into its own.The transmission function of the controller and voltage compensator is shown in Figure 5 (b).

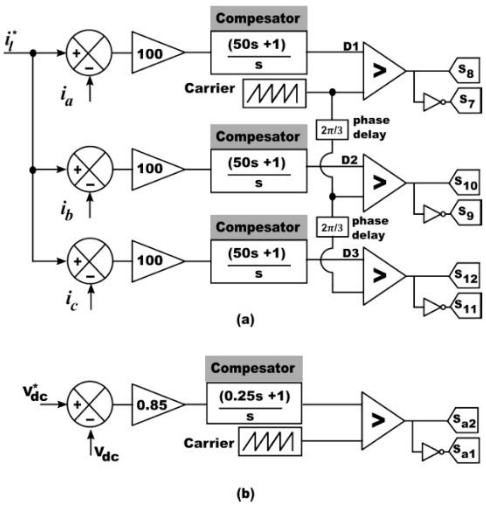

Fig.5 (a) Current control structure to implement IPWM for integrated interleaved dc-dc converter, (b) Voltage controller for regulating dc-link through battery side dc-dc converter.

Without adequate coordination between the three phases of power conversion, the suggested hybrid AC-DC charging system will not be able to work. The Type-2 AC charger, an active rectifier integrated into the vehicle, a bidirectional DC-DC converter on the battery side, and an interleaved DC-DC converter in the powertrain are all part of this process. Significant challenges include maintaining a steady DC-link voltage, controlling the AC charger's power operation, and charging the IDC in a regulated manner. An active rectifier is a common component in alternating current charging systems for regulation of the DC-link voltage and charging current. To interrupt the continuous power flow, combined AC-DC charging uses the same control mechanism. This is because adding DC input causes the total current to rise.We provide a coordinated control approach that divides up control duties to solve this problem. You may keep the DC-link voltage at 600 V by keeping the battery-connected DC-DC converter in voltage control mode. The onboard Type-2 AC charger may employ d-q management and continuous power mode to achieve UPU and UPF up to 19.4 kW. When connected to external DC sources, the IDC may convert to current control mode, enabling variable DC charging. By controlling the current on the d-axis using a PI-based power loop, the AC charger power may be kept constant and within rated limits. The IDC has an interleaved architecture that increases charging current and decreases ripple. A DC-link that is capable of receiving both AC and DC current is essential for AC-DC charging systems to function. To avoid control conflicts and circulating currents, the converter on the battery side absorbs all of the power, maintaining a constant voltage. By cooperating, we can keep the grid's power quality consistent, charge more rapidly, and make sure everything functions well.

TABLE I
SIMULATION PARAMETERS FOR THE PROPOSED COMBINATORY AC AND DC CHARGING OF EVS

Simulation Parameters	Value
Type-2 On-board AC charger	
Input three-phase ac voltage line to line	415 V
Output Power (P_{o1})	19.4 kW
line filter inductance (L_{ga}, L_{gb} & L_{gc})	1 mH/phase
Drivetrain inverter as interleaved DC-DC converter	
DC-Link Capacitor (C)	4700 μF
Motor and drivetrain Power rating	100 kW
DC link voltage (V_{dc})	600 V
DC input voltage range (V_{dc})	300-500 V
Motor winding inductance L_a, L_b & L_c	8 mH/phase
Battery dc-dc converter	
Battery voltages (Cutoff/Nominal/Full) (V_b)	325/450/550 V
Battery Ah	100 Ah
Filter inductor (L_1)	0.8 mH
Output capacitor (C_b)	1200 μF

The three-stage coordinated power conversion of the proposed hybrid AC-DC charging system consists of an onboard Type-2 active rectifier, an interleaved DC-DC converter (IDC) incorporated inside the engine, and a bidirectional DC-DC converter on the battery side. A central DC-link has made it much easier to transmit energy between the various converters. Keeping the AC charger switched on and ensuring a constant DC-link voltage are two crucial control challenges. Controlling the alternating current (AC) or direct current (DC) that goes into the batteries is still another crucial factor. Traditional alternating current (AC) charging systems use a battery-side converter to regulate current and an active rectifier to regulate DC-link voltage. Hybrid charging cannot be accomplished using this approach because of control problems, instability, and the loss of constant power functioning caused by the parallel DC input.A coordinated and decoupled control strategy is suggested to solve this problem. To maintain the DC-link voltage control mode at 600 V, the battery's DC-DC converter is responsible. In order to retain the unity power factor (UPF) while operating in continuous power management mode, the onboard AC charger limits its output below 19.4 kW. Depending on the availability of the source, the DC power injection may be adjusted using the current control mode of the IDC.

One way to get rid of control interference and circulating currents is to use several converters to deal with the DC-link voltage. A PI-based power loop controls the AC charger's power, and a zero-current on the q-axis keeps UPF constant. On the other hand, the current is shown on the d-axis. Both the interleaving differential converter and the battery-side converter improve DC charging, use all available power, and decrease interleaving current ripple. Because the converter on the battery side maintains a constant voltage and power balance, the DC-link may be powered by either AC or DC sources. These upgrades affect several facets of the system, including electrical quality, scalability, dependability, and efficiency.

IV. PROPOSED ANN CONTROLLER

In contrast to the more traditional Proportional-Integral (PI) controller, this project employs an ANN-based controller to regulate the converter system's output voltage and current. In contrast to conventional PI controllers, artificial neural network (ANN) controllers are able to learn and adapt to non-linear dynamics by training on system input-output data in a variety of load and grid configurations. This repair greatly reduces total harmonic distortion (THD) and improves the system's control precision, responsiveness to changes in circumstances, and power factor correction. The ANN-based method allows for more efficient regulation of dual-battery charging, more equitable power sharing, and robust operation in temporary situations. An ANN controller with many layers of back propagation is used to enhance the compensating device's performance. Using the MATLAB toolbox, we train the ANN. Levenberg-Marquardt-Backpropagation outperforms gradient-degressive and Gauss-Newton approaches for training the ANN controller. Competent learning, lower memory needs, and speedier convergence are just a few of the many benefits of the Levenberg-Marquardt back propagation approach [9]. The only data set used for training the ANN is the one belonging to the traditional PI controller. A single output layer, ten hidden layers, and two input levels make up the suggested controller for artificial neural networks. Both the original and updated error signals, which quantify the discrepancy between the real and reference values in the d and q coordinate systems, are sent into the ANN controller. A key principle of an ANN controller is to maximise accuracy while simultaneously minimising error. The work of converting the dqo data to abc format is being carried out by the ANN controller. Figure 6 shows that the ANN controller's performance metric is the mean square error. The difference between the intended and actual values is symbolised by this.

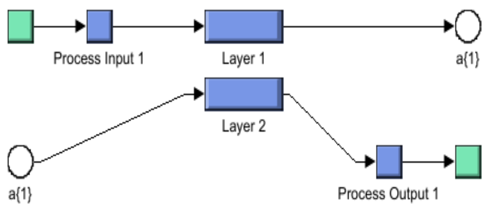

Fig.6 Typical Structure of ANN control

V.SIMULATION RESULTS

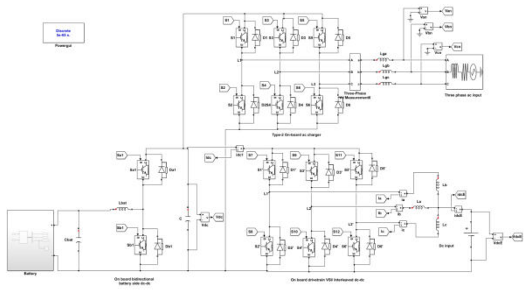

Fig.7 MATLAB/SIMULINK circuit of the system

The proposed combinatory AC–DC EV charging approach is simulated in MATLAB/Simulink.

A) EXISTING SIMULATION RESULTS

Figure 8 shows the results of applying the d-q technique to achieve unity power factor operating and regulate the onboard Type-2 AC charger. This control transforms the voltages and currents of the three-phase grid into components on the d- and q-axes, respectively. By controlling these settings, the PI controller keeps the input current in phase with the grid voltage. Chargers improve grid power quality when turned on by increasing the power factor near to one. Figure 9 depicts the control architecture of an integrated interleaved DC-DC converter that uses IPWM. In this case, the controller is responsible for controlling the amount of current passing through the converter's legs. Electric vehicle battery chargers that use interleaving may reduce current ripple and boost converter efficiency. This procedure involves distributing the current among the several branches of the converter. The DC-link voltage regulator and battery-side DC-DC converter are shown in Figure 10. The PI controller checks the current voltage against the DC-link reference voltage for every control signal. The DC-link voltage is maintained constant by this control, independent of whether AC and DC charging are occurring simultaneously.

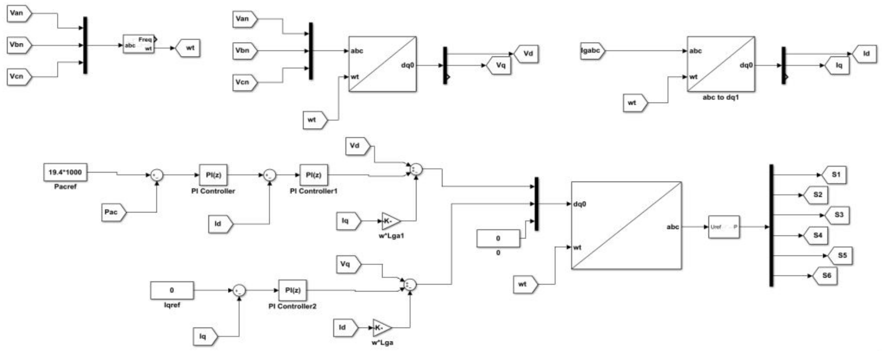

Fig.8 Controller for unity power factor operation for the onboard type-2ac charging using d − q control.

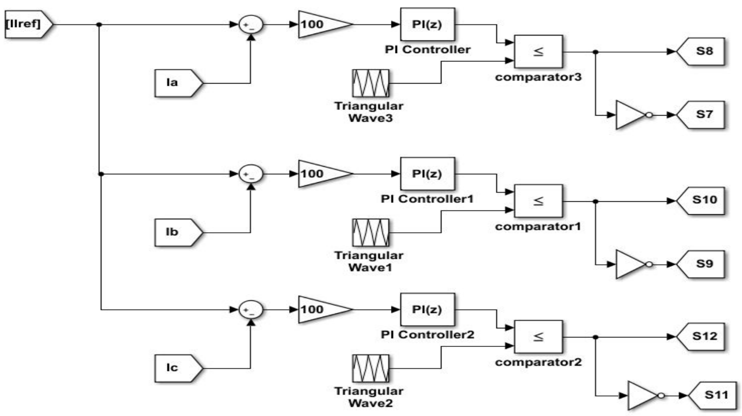

Fig.9 Current control structure to implement IPWM for integrated interleaved dc-dc converter

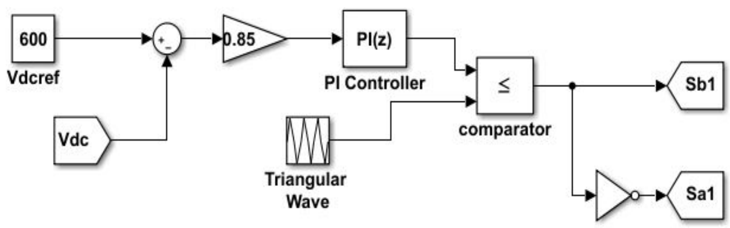

Fig.10 Voltage controller for regulating dc-link through battery side dc-dc converter.

In Figure 11, we can see the Type-2 charger's calculated grid currents and input phase voltages. For a better understanding of the phase voltages and currents, we also include the current waveforms scaled by a factor of 2.5 in addition to the phase voltages and currents (Van, Vbn, and Vcn). There is a unity power factor in the charger's operation because currents follow waveforms of voltage.

However, owing to the PI controller's imperfection, certain distortions and ripples may occur. At a charging rate of 1.6C, the three-leg interleaved DC-DC converter generates DC currents with high frequencies (as shown in Figure 12). The waveform is structured as follows: the base portion shows the external DC source voltage (VdcE), the top three legs show the converter currents (ia, ib, and ic), and the middle section shows the total input DC current (idcE). Consistent generation and maintenance of charging current throughout the interleaved converter's legs is possible, according to the results.You can see the voltage across the DC-link, the average power communicated by the Type-2 onboard charger, and the power from an external DC source in Figure 13, which shows both AC and DC charging running simultaneously. Combining AC and DC sources increases the charging rate, as can be seen from the chart. The DC-link voltage, however, has remained relatively unchanged.Figure 14 shows some features of the charging process, including power (Pbat), voltage (Vb), and current (Ibt). The findings reveal that the battery is charged using both AC and DC power sources. Thanks to the PI controller's dynamics, the charging current is somewhat unexpected, but the system still works well.

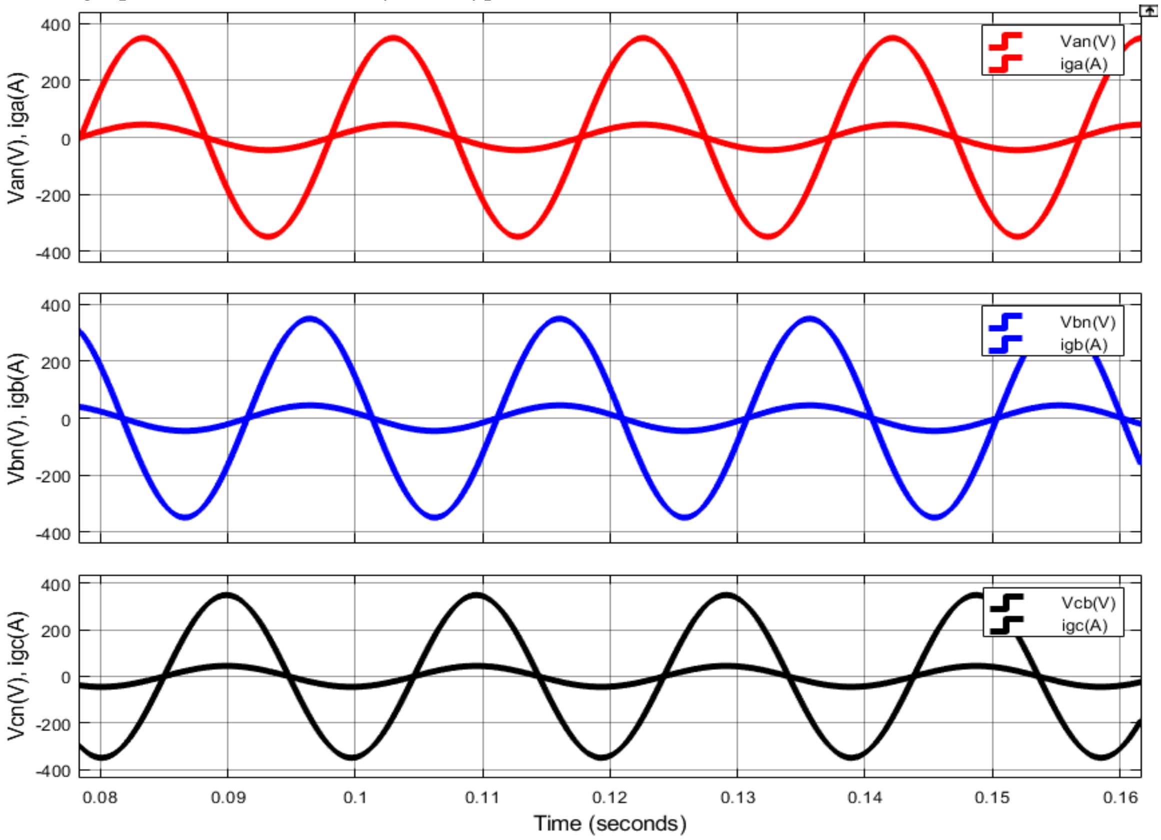

Fig. 11. During the simulation, the input phase voltages and currents of the Type-2 charger are (Van, Vbn, Vcn) (V) and (Iga, Igb, Igc) (A), with the phase currents being twice as large.

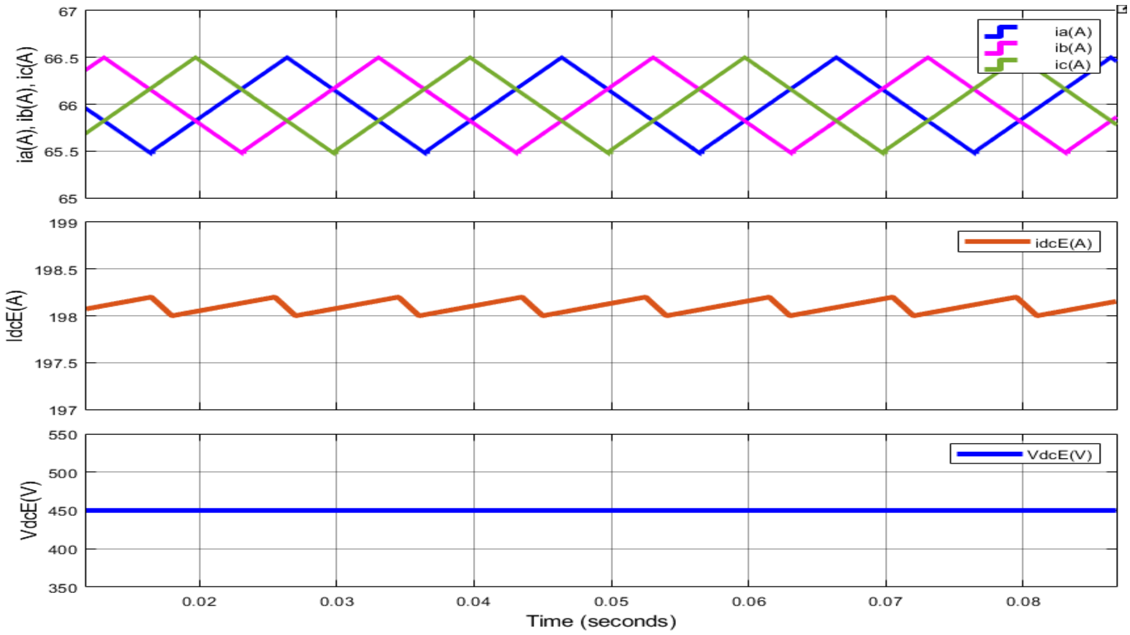

Fig. 12The outcomes of the simulation allow us to observe: (a) idcE, the overall input direct current, as seen in the middle trace; (iv) VdcE, the voltage of the external direct current source; and (a), A, the high frequency direct currents of the three legs of the interleaved direct current converter (ia, ib, and ic), for an electric vehicle (EV) battery charging rate of 1.6C.all the way down.

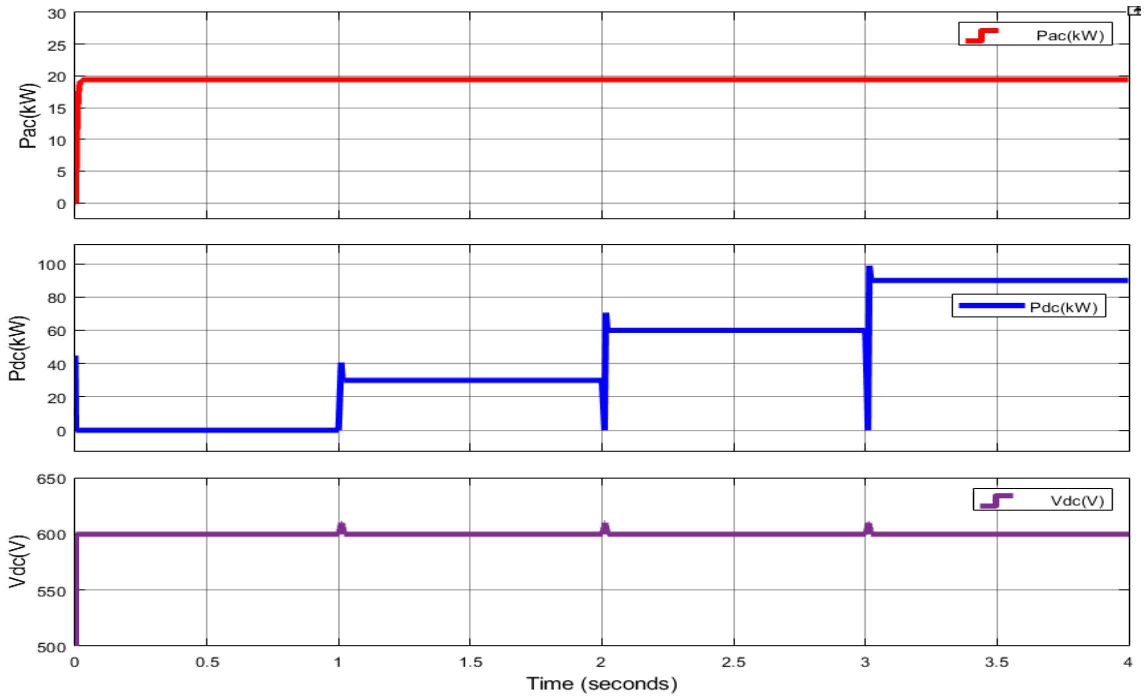

Fig.13The top trace displays the average power transferred via Type-2 OBC (Pac) (kW), the middle trace displays the input DC current (kW), and the bottom trace displays the voltage across the dc-link (Vdc) (V) throughout full alternating current and direct current charging.

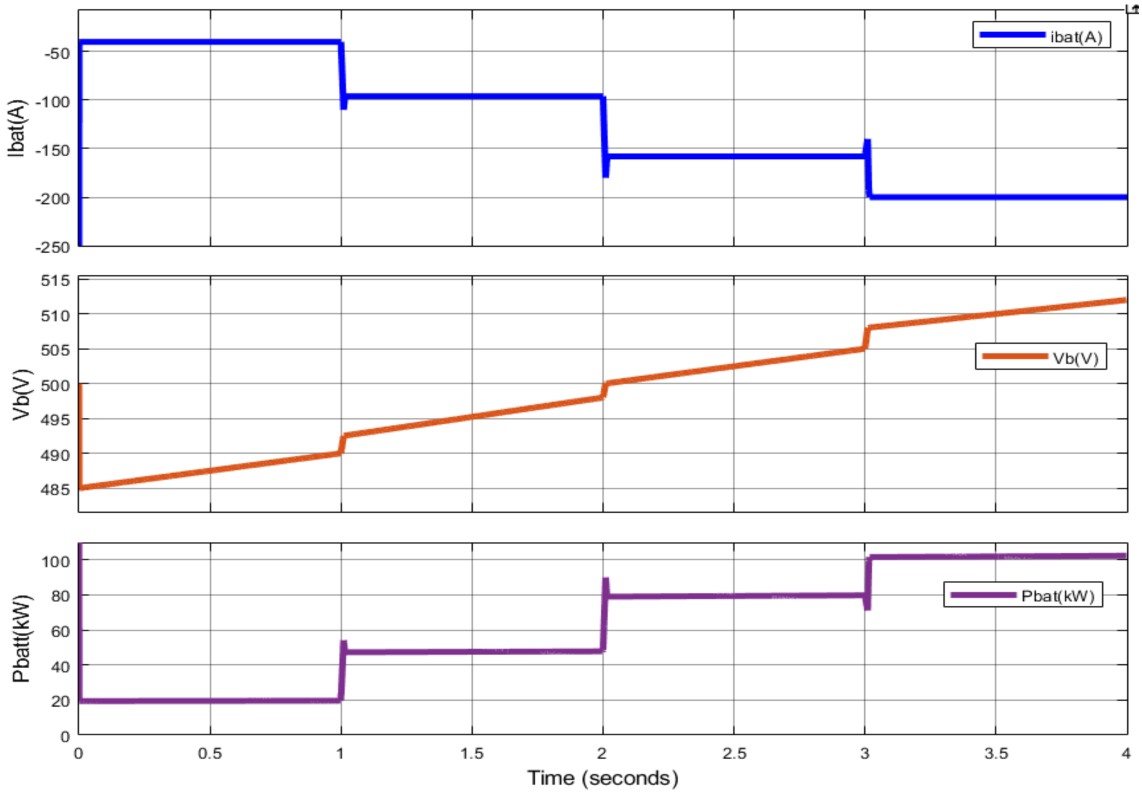

Fig. 14. While conducting charging using alternating current and direct current, the simulation results show the following: terminal voltage (Vb) in volts (V), current (Ibt) in kilowatts (kW), and power (Pbat) in kW.

B) EXTENSION SIMULATION RESULTS

Figure 15 shows the proposed new controller for unity power factor operation, which replaces the conventional PI controller. For this, an ANN is used. The ANN controller enhances the overall performance of the Type-2 onboard charger by making the d-q control framework more responsive and accurate in regulating current. In Figure 16, we can see an ANN controller-based approach to controlling the current in an interleaved DC-DC converter. With ANN-based converter leg control, sharing is improved and current monitoring is more accurate. This means there is less ripple and better efficiency when the converter charges the batteries. As indicated in Figure 17, the voltage controller is responsible for regulating the DC-link voltage. Because of its improved voltage management and faster response time, the ANN controller guarantees a more stable DC-link voltage during combined charging operation than a typical PI controller.

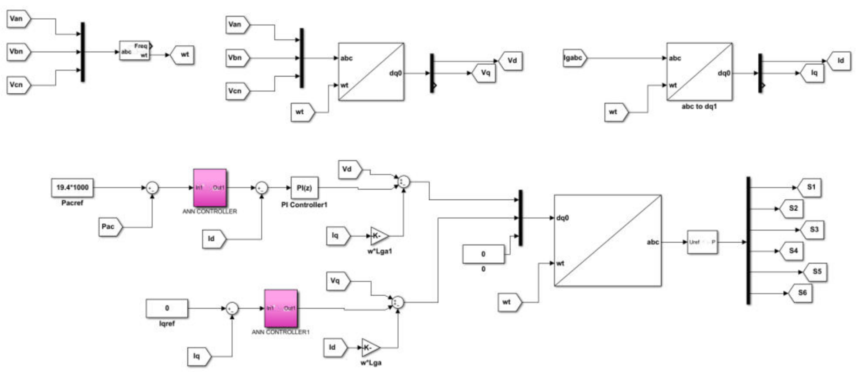

Fig.15 Proposed Controller for unity power factor operation for the onboard type-2ac charging using d − q control.

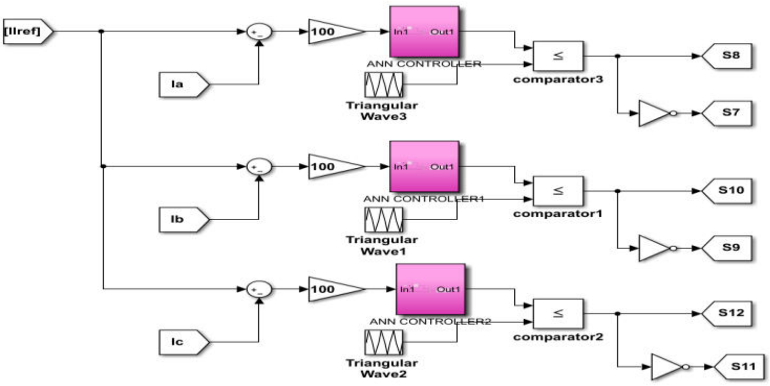

Fig.16 Proposed Current control structure to implement IPWM for integrated interleaved dc-dc converter

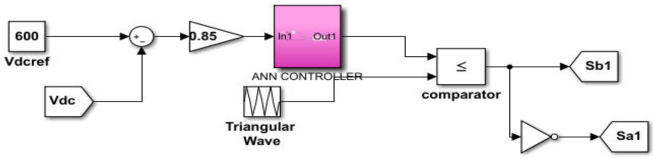

Fig.17 Proposed Voltage controller for regulating dc-link through battery side dc-dc converter.

Figure 18 displays the output of the suggested ANN-based system's simulation of grid currents and input phase voltages. In contrast to square-shaped voltage waves, the pattern of grid currents is more sinusoidal. Power factor adjustment and harmonic distortion have both been enhanced in comparison to the previous system that was controlled by PI. Figure 19 shows, with the aid of an artificial neural network, the total DC input current, external DC source voltage, and high-frequency DC currents flowing through the interleaved converter legs. The charging process is made more effective and dependable by spreading the current out more evenly throughout the legs of the converter and decreasing ripple. In Figure 20, we can see how the DC-link voltage and an external DC source provide power to the AC charger. Charging becomes more efficient with the help of the ANN controller, which can stabilise the DC-link voltage and improve coordination between the AC and DC power sources. The charging power, voltage, and current are shown in Figure 21. There are fewer dips and a more consistent charging profile compared to the PI controller. With the help of the ANN-based control mechanism, the overall performance of the system and charging stability are both enhanced.

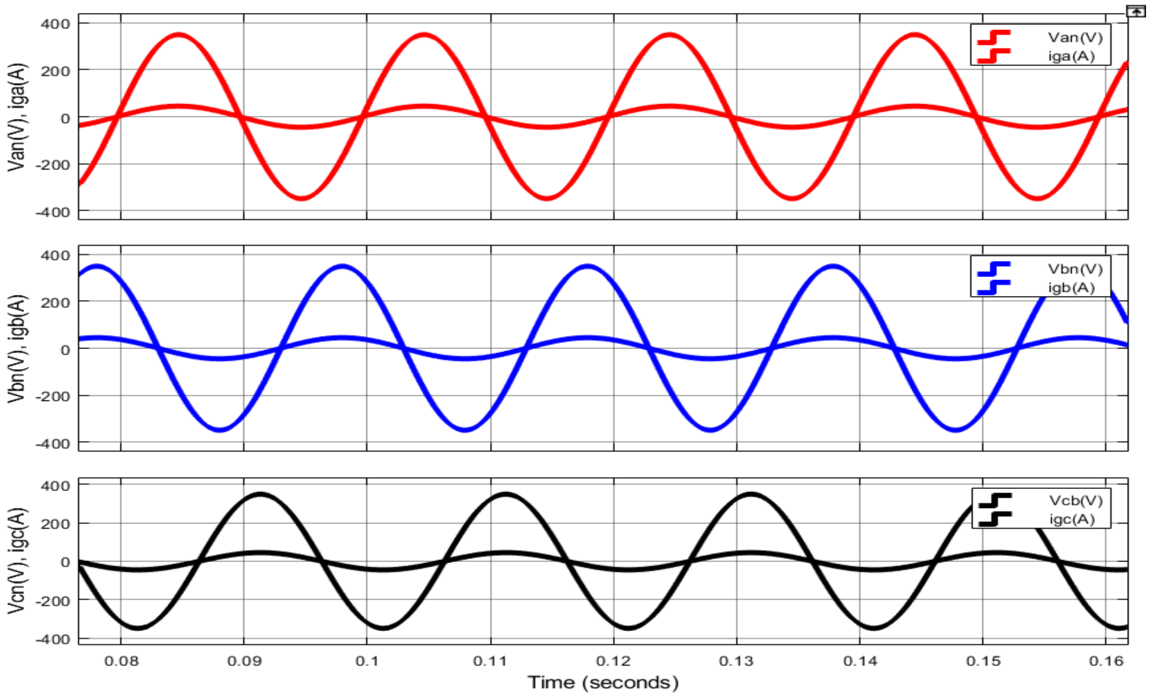

Fig.18. The input phase voltages and currents (Van, Vbn, Vcn) (V) and (Iga, Igb, Igc) (A) of the Type-2 charger are shown in the suggested model, with phase currents being multiplied by 2.5.

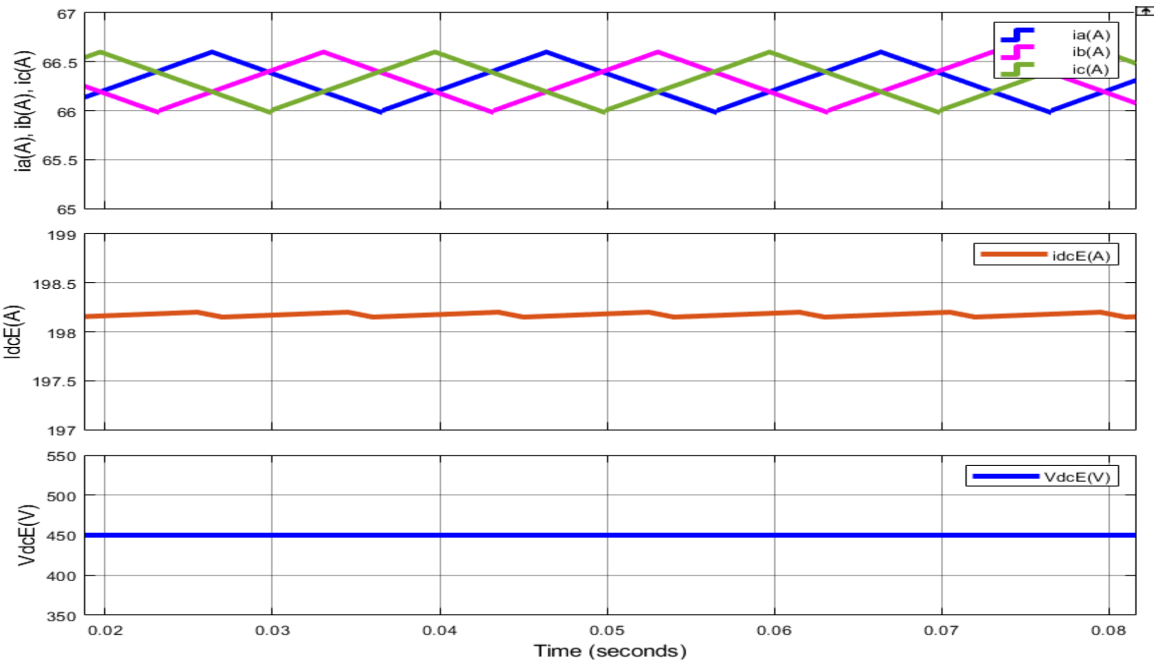

Fig. 19. Proposed Based on the simulation results, we can see: (a) idcE, the total input direct current, as shown by the middle trace, For an electric vehicle (EV) battery charging rate of 1.6C, (iv) VdcE, the voltage of the external direct current source; and (a), A, the high frequency direct currents of the three legs of the interleaved direct current converter (ia, ib, and ic).on the bottom.

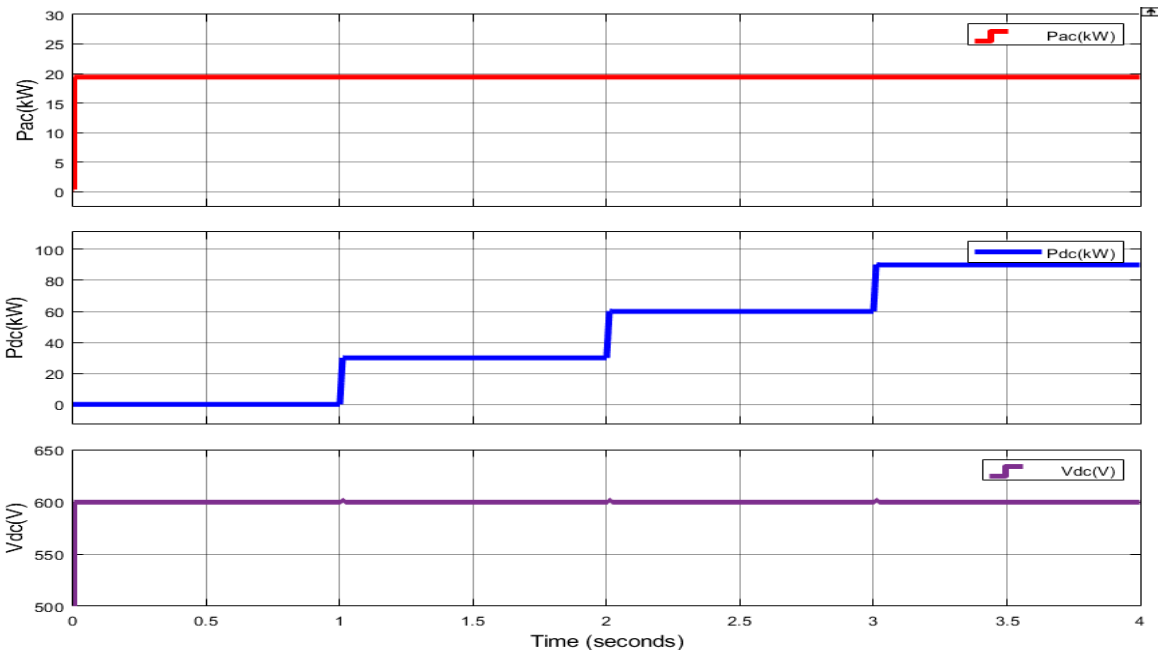

Fig. 20. Power transferred via the Type-2 OBC (Pac) in kW, power transmitted over the IDC (Pdc) in kW, and voltage across the dc-link (Vdc) in V are the usual outcomes of the simulation for the combined ac and dc charging process.

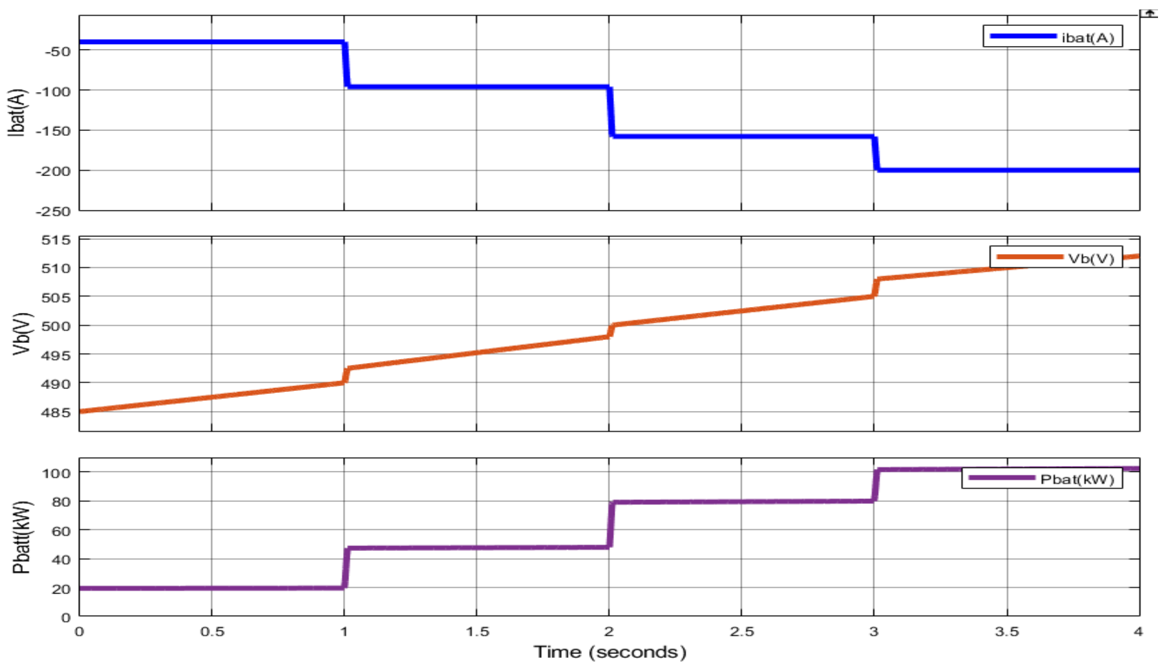

Fig. 21. The suggested simulation results display the following: power (Pbat) (kW), terminal voltage (Vb) (V), and current (Ibt) (kW) during combined ac and dc charging of the battery.

The ANN-based control technique considerably enhances system performance, as compared with the PI controller. The advantages include more constant charging profiles for batteries, less current ripple, better control of the DC-link voltage, and more efficient power sharing between AC and DC sources. This leads to quicker dynamic reaction and improved charge efficiency for the suggested ANN controller.

COMPARISION TABLE

Parameter	Existing System (PI Controller)	Extension System (ANN Controller)
Input current waveform	Noticeable ripple	Smoother and more sinusoidal
Interleaved current ripple	Higher ripple in leg currents	Reduced ripple and better current sharing
DC-link voltage stability	Minor fluctuations	Improved voltage regulation
Power sharing (AC + DC)	Less uniform	More stable and balanced
Battery charging current	More oscillations	More stable charging profile
Battery charging performance	Moderate efficiency	Improved dynamic response

CONCLUSION

To enhance the charging speed of electric car batteries, this study offers a hybrid AC-DC charging approach. Put the Type-2 on-board charger into continuous power mode and the drivetrain inverter into current control mode to use both the on-board AC-DC converter and the DC-DC converter included into the drivetrain. In place of the conventional PI controller, an ANN-based controller is used to better regulate the shared DC-link voltage and to synchronise the power transfer between the AC and DC charging channels. Another option is to utilise the DC-DC converter that is connected to the batteries for this. The enhanced system stability and responsiveness in a variety of operating circumstances may be attributed to the ANN controller's capacity to learn from its past mistakes. Electric cars' built-in motors and drivetrains make high-power DC charging possible, allowing for a faster charging rate with a more powerful DC source. The results of the experiments and the calculations suggest that the 2C charging rate has a better window. Results from tests demonstrate that the system can handle combined AC-DC charging with ease, as well as 19 kW AC charging, 30 kW DC charging, 60 kW DC charging, and 90 kW DC charging within the input voltage range of 250-450 V DC.

REFERENCES

[1]A. G. Boulanger, A. C. Chu, S. Maxx, and D. L. Waltz, "Vehicle electri- fication: Status and issues," Proc. IEEE, vol. 99, no. 6, pp. 1116–1138 Jun. 2011.

[2]H. Tu, H. Feng, S. Srdic, and S. Lukic, "Extreme fast charging of electric vehicles: A technology overview," IEEE Trans. Transport. Electrific.,vol. 5, no. 4, pp. 861–878, Dec. 2019.

[3] M. Yilmaz and P. T. Krein, "Review of battery charger topologies, charging power levels, and infrastructure for plug-in electric and hybrid vehicles," IEEE Trans. Power Electron., vol. 28, no. 5, pp. 2151–2169, May 2013.

[4] L. Tan, B. Wu, V. Yaramasu, S. Rivera, and X. Guo, "Effective voltage balance control for bipolar-DC-bus-fed EV charging station with three- level DC–DC fast charger," IEEE Trans. Ind. Electron., vol. 63, no. 7, pp. 4031–4041, Jul. 2016, doi: 10.1109/TIE.2016.2539248.

[5] L. Solero, "Nonconventional on-board charger for electric vehicle propulsion batteries," IEEE Trans. Veh. Technol., vol. 50, no. 1, pp. 144–149, Mar. 2001.

[6] S.-K. Sul and S.-J. Lee, "An integral battery charger for four-wheel drive electric vehicle," IEEE Trans. Ind. Appl., vol. 31, no. 5, pp. 1096–1099, Oct. 1995.

[7] S. R. Meher, S. Banerjee, B. T. Vankayalapati, and R. K. Singh, "A reconfigurable on-board power converter for electric vehicle with reduced switch count," IEEE Trans. Veh. Technol., vol. 69, no. 4, pp. 3760–3772, Apr. 2020, doi: 10.1109/TVT.2020.2973316.

[8] S. Wang and P. W. Lehn, "Design and control of 3-phase integratedcharger for dual-inverter drivetrain electric vehicles," in Proc. IEEE Transp. Electrific. Conf. Expo. (ITEC), Detroit, MI, USA,

Jun. 2019, pp. 1–6, doi: 10.1109/ITEC.2019.8790589.

[9] F. Lacressonniere and B. Cassoret, "Converter used as a battery charger and a motor speed controller in an industrial truck," in Proc. Eur. Conf.Power Electron. Appl., Sep. 2005, p. 7.

[10] S. Lacroix, E. Laboure, and M. Hilairet, "An integrated fast battery charger for electric vehicle," in Proc. IEEE Vehicle Power Propuls. Conf., Sep. 2010, pp. 1–6, doi: 10.1109/VPPC.2010.5729063.

[11] H. J. Raherimihaja, Q. Zhang, T. Na, M. Shao, and J. Wang, "A three-phase integrated battery charger for EVs based on six-phase open- end winding machine," IEEE Trans. Power Electron., vol. 35, no. 11, pp. 12122–12132, Nov. 2020, doi: 10.1109/TPEL.2020.2986798.

[12] S. Sharma, M. V. Aware, and A. Bhowate, "Integrated battery charger for EV by using three-phase induction motor stator windings as filter," IEEE Trans. Transport. Electrific., vol. 6, no. 1, pp. 83–94, Mar. 2020.

[13] S. Ranjith, V. Vidya, and R. S. Kaarthik, "An integrated EV battery charger with retrofit capability," IEEE Trans. Transport. Electrific., vol. 6, no. 3, pp. 985–994, Sep. 2020, doi: 10.1109/TTE.2020.2980147.

[14] I. Subotic, N. Bodo, E. Levi, and M. Jones, "Onboard integrated battery charger for EVs using an asymmetrical nine-phase machine," IEEE Trans. Ind. Electron., vol. 62, no. 5, pp. 3285–3295, May 2015.

[15] C. Viana and P. W. Lehn, "A drivetrain integrated DC fast charger with buck and boost functionality and simultaneous drive/charge capability," IEEE Trans. Transport. Electrific., vol. 5, no. 4, pp. 903–911, Dec. 2019, doi: 10.1109/TTE.2019.2925211.

[16] S. Loudot, B. Briane, L. Ploix, and A. Villeneuve, "Fast charging device for an electric vehicle," U.S. Patent 20 120 286 740 A1, Nov. 15, 2012.

[17] C. Viana, M. Keshani, and P. W. Lehn, "Interleaved buck-boost inte- grated DC fast charger with bidirectional fault blocking capability," in Proc. 20th Workshop Control Modeling Power Electron. (COMPEL), Jun. 2019, pp. 1–7.

[18] R. Shi, S. Semsar, and P. W. Lehn, "Constant current fast charging of electric vehicles via a DC grid using a dual-inverter drive," IEEE Trans. Ind. Electron., vol. 64, no. 9, pp. 6940–6949, Sep. 2017.

[19] V. T. Tran, Md. R. Islam, K. M. Muttaqi, and D. Sutanto, "An efficientenergy management approach for a solar-powered EV battery charging facility to support distribution grids," IEEE Trans. Ind. Appl., vol. 55, no. 6, pp. 6517–6526, Nov. 2019, doi: 10.1109/TIA.2019.2940923.

[20] A. Dubey and S. Santoso, "Electric vehicle charging on residential distribution systems: Impacts and mitigations," IEEE Access, vol. 3, pp. 1871–1893, 2015.

[21] U. B S, V. Khadkikar, H. H. Zeineldin, S. Singh, H. Otrok, and R. Mizouni, "Direct electric vehicle to vehicle (V2V) power trans- fer using on-board drivetrain and motor windings," IEEE Trans. Ind. Electron., vol. 69, no. 11, pp. 10765–10775, Nov. 2022, doi: 10.1109/TIE.2021.3121707.

[22] M. Shurrab, S. Singh, H. Otrok, R. Mizouni, V. Khadkikar, and H. Zeineldin, "A stable matching game for V2V energy sharing—A user satisfaction framework," IEEE Trans. Intell. Transp. Syst., vol. 23, no. 7, pp. 7601–7613, Jul. 2022, doi: 10.1109/TITS.2021.3071449.